Applied Science and Engineering Progress, Vol. 20, No. 2, 2027, 8264

Research Article

Development of Core-Shell Alginate-Gelatin Capsules for Stabilization of Kratom Alkaloids via Coaxial Electrospray

Chutatip Tongped, Apisittipong Srinusud, Lida Simasatitkul, Samitthichai Seeyangnok, and Nisalak Trongsiriwat*
Department of Industrial Chemistry, Faculty of Applied Science, King Mongkut's University of Technology North Bangkok, Bangkok, Thailand

Itthipol Sungwienwong
Department of Chemistry, Faculty of Science, Srinakharinwirot University, Bangkok, Thailand

* Corresponding author. E-mail: nisalak.t@sci.kmutnb.ac.th DOI: 10.14416/j.asep.2026.08.005
Received: 5 May 2026; Revised: 18 June 2026; Accepted: 28 June 2026; Published online: 17 August 2026

Abstract
Kratom (*Mitragyna speciosa* Korth.) contains bioactive alkaloids, particularly mitragynine, which exhibit poor aqueous solubility and instability under light and thermal conditions, limiting their practical applications. This study presents a process-oriented approach for stabilizing kratom extract via core–shell encapsulation using a coaxial electrospray technique. Gelatin and sodium alginate were employed as core and shell materials, respectively. The effects of sodium alginate concentration (1.0–2.0 % w/v) and applied voltage (0–2,500 V) on capsule morphology and size distribution were systematically investigated. Optimal conditions (2.0 % w/v alginate, 1,500 V) yielded uniform spherical capsules with an average diameter of 4.29 ± 0.07 mm. Structural characterization using FT-IR confirmed successful encapsulation, while UV–Vis and GC–MS analyses verified the presence and quantified the content of mitragynine. Stability studies demonstrated that capsules maintained structural integrity under neutral pH and varied temperature conditions over 14 days. Cytotoxicity evaluation using Vero cells indicated high cell viability (> 80 %), confirming biocompatibility. The results highlight the feasibility of coaxial electrospray as a scalable and controllable encapsulation process for bioactive compounds in food and pharmaceutical engineering applications.

Keywords: Alginate, Coaxial Electrospray, Encapsulation, Kratom, Stability

1 Introduction

Kratom (*Mitragyna speciosa* Korth.) is a tropical medicinal plant widely used throughout Southeast Asia, particularly in Thailand, Malaysia, Indonesia, and the Philippines [1]. Its pharmacological activity is primarily associated with a complex mixture of indole alkaloids, with more than 25 compounds identified to date [2]. Among these, mitragynine, Figure 1, is the major alkaloid constituent, accounting for approximately 66 % of the total alkaloid content [3]. Other important alkaloids, including speciogynine, speciociliatine, and mitraciliatine, are structural diastereomers of mitragynine that exhibit analgesic activity through interactions with opioid receptors [4]. In addition, previous animal studies have reported that 7-hydroxymitragynine exhibits substantially stronger antinociceptive activity than mitragynine and morphine under specific experimental conditions [5]. These pharmacological properties have attracted increasing interest in the potential application of kratom-derived compounds in pharmaceutical, nutraceutical, and functional food systems.

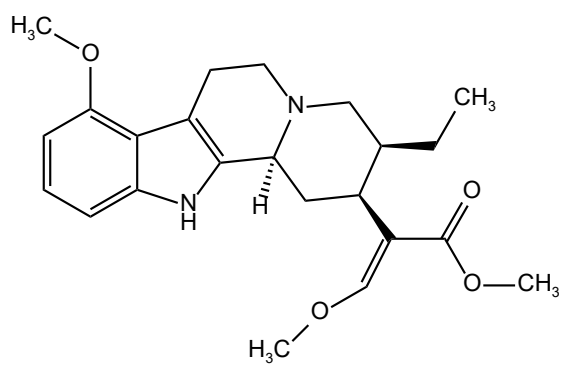

Figure 1: Structure of mitragynine.

Applied Science and Engineering Progress, Vol. 20, No. 2, 2027, 8264

Despite these promising bioactivities, the practical application of kratom extract remains challenging due to the poor aqueous solubility, photodegradation sensitivity, and thermal instability of its active alkaloids, particularly mitragynine. These physicochemical limitations can reduce formulation stability, decrease bioactive retention during storage, and hinder precise dosage control. Therefore, the development of an effective encapsulation system is necessary to improve the stability, protection, and delivery efficiency of kratom-derived bioactive compounds.

Encapsulation technologies have been widely explored as effective approaches for enhancing the stability and controlled delivery of sensitive bioactive compounds. Among these techniques, coaxial electrospray has gained considerable attention due to its ability to produce core–shell particles through a single-step process with precise control over particle morphology, shell thickness, and encapsulation structure (Figure 2) [6]. In coaxial electrospray, the application of an electric field generates a stable Taylor cone, enabling controlled droplet formation and fabrication of tunable core–shell capsules [7]. Compared with conventional encapsulation methods, coaxial electrospray offers advantages including mild processing conditions, reduced thermal stress, and compatibility with biopolymer-based systems [8].

In this study, sodium alginate and gelatin were selected as shell and core materials, respectively, due to their complementary physicochemical properties and synergistic functionality in core–shell encapsulation systems. Sodium alginate is a biocompatible and biodegradable polysaccharide capable of rapid ionic gelation with calcium ions, enabling formation of mechanically stable hydrogel shells with good structural integrity [9], [10]. In addition, alginate exhibits excellent film-forming ability and mild gelation behavior, making it highly suitable for electrospray-based encapsulation processes [11]. Gelatin, a natural amphiphilic biopolymer derived from collagen, possesses favorable film-forming properties, high biocompatibility, and the ability to interact with hydrophobic bioactive compounds, making it an appropriate matrix for the incorporation of kratom extract [12]. The combination of alginate and gelatin provides several synergistic advantages, including improved encapsulation efficiency, enhanced mechanical stability, reduced leakage of sensitive compounds, and increased protection against environmental stress [13].

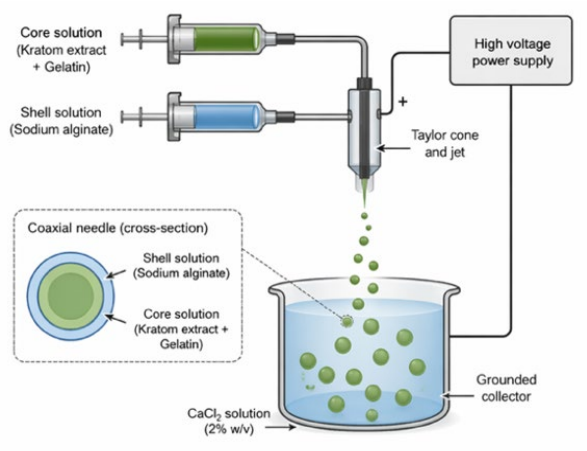

Figure 2: Schematic diagram of the coaxial electrospray for core-shell capsule preparation.

Although previous studies have investigated kratom alkaloids and their potential pharmaceutical applications, most reports have primarily focused on extraction, phytochemical characterization, and biological activity evaluation rather than advanced encapsulation strategies [14], [15]. Recent studies have explored formulation approaches such as nanostructured lipid carriers [16] and microencapsulation systems [17] for improving kratom extract delivery and stability. However, these systems were mainly developed using conventional encapsulation techniques and did not provide precise control over core–shell structure, capsule morphology, or electrospray-mediated particle formation. In addition, challenges related to physicochemical stability and protection of sensitive alkaloids during processing and storage remain insufficiently addressed. In contrast, coaxial electrospray offers several advantages, including mild single-step fabrication, controllable core–shell morphology, reduced thermal stress, and improved structural protection of encapsulated bioactive compounds. Therefore, this study aimed to develop and optimize an alginate–gelatin core–shell encapsulation system for kratom extract using coaxial electrospray.

To the best of our knowledge, this is among the first studies to apply a coaxial electrospray alginate–gelatin core–shell system for kratom extract encapsulation and stabilization**.** In addition, this study systematically investigates the effects of sodium alginate concentration and applied voltage on capsule morphology and size distribution, while also evaluating environmental stability, mitragynine content, and cytocompatibility. The findings provide important insight into the development of

biopolymer-based protective encapsulation systems for kratom-derived bioactive compounds and establish a foundation for future pharmaceutical, nutraceutical, and cosmetic applications.

2 Materials and Methods

2.1 *Materials*

Dried kratom leaves (*Mitragyna speciosa* Korth.) Havil. were obtained from a local supplier in Thailand. Food-grade ethanol (95 %), gelatin, sodium alginate, and calcium chloride were purchased from Krungthepchemi, Thailand. Analytical-grade methanol (99.8 %) and dimethyl sulfoxide (DMSO) were procured from Merck KGaA (Germany). The mitragynine reference standard was used for UV-Vis calibration. Type II ultra-pure water was used throughout. Vero cells were supplied by the Biotechnology Center, King Mongkut's University of Technology North Bangkok. MTT (3-(4,5-dimethylthiazol-2-yl)-2,5-diphenyltetrazolium bromide) was used for cytotoxicity assays.

2.2 *Extraction of kratom*

Dried kratom leaves were pulverized and subjected to solvent extraction using 95% ethanol at ambient temperature. The extraction was performed in a sealed system for 72 h and repeated three consecutive times with fresh solvent to maximize yield. The combined extracts were filtered and subsequently concentrated under reduced pressure using a rotary evaporator (50 °C, 200 mbar, 100 rpm) until a viscous crude extract was obtained. The extract was stored in light-protected containers at 4 °C until further use.

2.3 *Coaxial electrospray encapsulation*

Encapsulation was carried out using a coaxial electrospray setup (BUCHI B-390) using a concentric nozzle configuration comprising an outer nozzle (900 µm inner diameter) and an inner nozzle (750 µm inner diameter). The inner phase was prepared by dispersing kratom extract and gelatin at a ratio of 1:1.5 in ultrapure water to obtain a homogeneous solution. The outer phase was prepared by dissolving sodium alginate at concentrations of 1.0–2.0% (w/v), followed by thermal stirring and degassing to eliminate air bubbles. During processing, the core and shell solutions were simultaneously delivered through concentric nozzles into a 500 mL calcium chloride crosslinking bath (2% w/v), enabling immediate gelation of the alginate shell and formation of core–shell capsules.

2.3.1 Optimization of sodium alginate concentration

Shell sodium alginate concentration was varied at 1.0, 1.5, and 2.0 % w/v, with fixed parameters: core flow rate 28 mL/h, shell flow rate 52 mL/h, voltage 500 V, frequency 40 Hz, and air pressure 600 mbar. Capsule morphology and encapsulation quality were evaluated visually and by size analysis.

2.3.2 Optimization of applied voltage

Using the optimal sodium alginate concentration (2.0 % w/v), the applied voltage was varied at 0, 500, 1,000, 1,500, and 2,500 V, while maintaining all other parameters constant. Optimal voltage was selected based on capsule sphericity, core centration, and structural completeness.

2.4 *Particle size analysis*

Approximately 25 capsules from each condition were photographed alongside a calibrated scale ruler. Capsule diameters were measured using ImageJ software and reported as mean ± standard deviation.

2.5 *UV-Vis spectroscopy*

Mitragynine reference standard and crude kratom extract were dissolved in ethanol and scanned over 190–800 nm using a UV-Visible Spectrophotometer (SPECORD 210 PLUS, Analytik Jena, Germany) to confirm the presence of mitragynine via characteristic absorption peaks. A calibration curve was constructed from kratom extract solutions at 5, 10, 15, 20 and 25 ppm measured at 225 nm.

2.6 *Fourier transform infrared spectroscopy*

FT-IR spectra of the kratom extract, sodium alginate, and prepared boba capsules were recorded using a Perkin-Elmer Spectrum 100 FT-IR spectrometer (USA) over 4,000–400 cm^{-1}. Samples were ground with KBr and pressed into pellets. Spectra were compared to confirm encapsulation and identify characteristic functional groups.

Applied Science and Engineering Progress, Vol. 20, No. 2, 2027, 8264

2.7 *Stability testing of boba capsules*

Capsule stability was evaluated under three conditions: (i) pH 1–10 buffer solutions at days 1, 7, and 14; (ii) ultra-pure water versus 2 % w/v calcium chloride solution at room temperature and 4 °C for 14 days. Capsule size and physical appearance were monitored at each time point using ImageJ analysis.

2.8 *Mitragynine quantification*

The composition of crude kratom extract was determined by GC-MS (Agilent 7890B; HP-5MS column; temperature ramp 100–300 °C at 10 °C/min; split ratio 20:1; flow rate 1 mL/min). Mitragynine content was calculated from peak area integration. For capsule content, 10 capsules were dissolved in ethanol and the absorbance at 225 nm was substituted into the UV-Vis calibration equation to determine total extract concentration. Mitragynine mass per capsule was calculated using the GC-MS-derived alkaloid fraction.

2.9 *Cytotoxicity assay*

Crude kratom extract was dissolved in DMSO (10 mg/mL) and sterilized by filtration through a 0.2-µm membrane. Serial dilutions (0.3125–10 µg/mL) were prepared and tested against Vero cells using the MTT assay. Cells were incubated at 37 °C for 3 h with MTT reagent; formazan crystals were dissolved in DMSO and absorbance measured at 570 nm. Cell viability (%) relative to untreated controls was calculated.

2.10 *Statistical analysis*

All experiments were performed in triplicate, and results are presented as mean ± standard deviation (SD). Statistical analysis was conducted using IBM SPSS Statistics (Version 28.0, IBM Corp., Armonk, NY, USA). Differences among groups were evaluated using one-way analysis of variance (ANOVA), followed by an appropriate post-hoc multiple comparison test. Statistical significance was considered at p-value < 0.05.

3 Results and Discussion

3.1 *Process optimization*

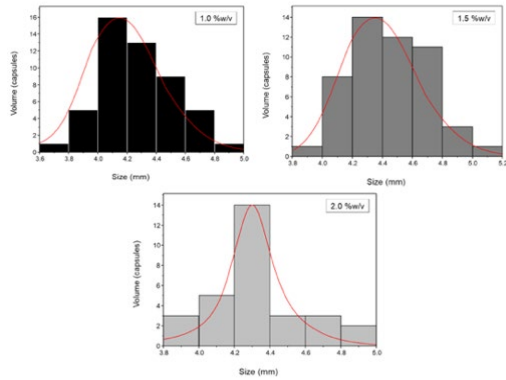

Figure 3 : Size distribution of capsules with sodium alginate 1.0, 1.5 and 2.0% w/v.

3.1.1 Effect of alginate concentration

The morphology of the capsules was strongly influenced by sodium alginate concentration through its effect on solution viscosity and electrospray jet stability. As shown in Table 1, low alginate concentrations (1.0–1.5% w/v) provided insufficient polymer chain entanglement, resulting in reduced viscosity, unstable jet formation, incomplete shell development, and off-center core positioning. Increasing the alginate concentration to 2.0% (w/v) enhanced viscoelastic forces and promoted stable Taylor cone formation, producing spherical core–shell capsules with centrally positioned cores and the most uniform size distribution (Figure 3). The higher viscosity increased resistance to electrostatic deformation, thereby stabilizing the coaxial jet and improving shell formation. The size distribution histograms further demonstrated that increasing alginate concentration improved capsule size homogeneity. The 2.0% (w/v) formulation exhibited a narrower distribution profile and greater clustering of capsule diameters around the mean value than the1.0% and 1.5% (w/v) formulations, indicating improved reproducibility of capsule formation. In contrast, broader distributions at

Table 1 : Capsule size at different sodium alginate concentrations.

Alginate (% w/v)	Mean size* (mm)	Morphology
1.0	4.4468 ± 0.34[a]	Incomplete, fused
1.5	4.4366 ± 0.10 [a]	Partial, off-center
2.0	4.2910 ± 0.07 [a]	Complete, spherical

**Values are presented as the mean ± SD (n = 3). Means sharing the same superscript letters are not significantly different (p-value > 0.05).*

lower alginate concentrations suggest greater variability in droplet breakup and shell formation due to insufficient viscosity. Similar observations have been reported in previous alginate-based electrospray studies, where increasing polymer concentration improved capsule sphericity and reduced size variability. The behavior observed in the present study is consistent with these findings, confirming that enhanced polymer chain entanglement and solution viscosity contribute to improved jet stability and core–shell formation. Although the absolute capsule size depends strongly on nozzle geometry and operating conditions, the morphology development trend observed here agrees well with previous electrospray studies [8].

Although the 2.0% (w/v) formulation produced superior morphology and size uniformity, statistical analysis revealed no significant differences in mean capsule diameter among the tested alginate concentrations (p-value > 0.05). This is likely attributable to the fixed coaxial nozzle configuration (outer nozzle diameter = 900 μm; inner nozzle diameter = 750 μm), which largely governed droplet size during electrospray generation. Therefore, while alginate concentration significantly affected capsule morphology, shell integrity, and encapsulation quality, its influence on the final capsule diameter was limited. Consequently, formulation optimization was based primarily on core–shell structure, morphological integrity, and size uniformity rather than diameter alone.

3.1.2 Effect of applied voltage

The applied voltage markedly influenced capsule morphology by governing droplet formation and jet stability during the coaxial electrospray process. As shown in Table 2, insufficient electrostatic force at 0 V resulted in deformed capsules without distinct core–shell structures, while intermediate voltages (500–1,000 V) improved capsule formation but still produced eccentric core positioning and irregular shell morphology. The optimal voltage of 1,500 V generated a stable Taylor cone, enabling balanced electrostatic and surface tension forces that produced spherical capsules with centrally positioned cores and a narrow size distribution (4.36 ± 0.22 mm; Figure 4). The size distribution histograms further supported the effect of voltage on capsule formation. Capsules produced at 1,500 V exhibited the narrowest and most symmetrical distribution profile, indicating improved size homogeneity and process reproducibility. In contrast, broader distributions were observed at lower voltages (0–1,000 V), reflecting greater variability in droplet formation due to insufficient electrostatic force. At 2,500 V, the histogram showed a broader and partially bimodal distribution, suggesting jet instability and inconsistent droplet breakup under excessive electric field strength. In contrast, excessive voltage (2,500 V) caused jet instability, shell rupture, and leakage of the encapsulated core material. These findings are consistent with electrospray theory, in which capsule morphology is governed by the interplay between electric field strength, fluid properties, and flow conditions [18].

Although voltage significantly affected capsule morphology and encapsulation quality, statistical analysis revealed no significant differences in mean capsule diameter among the voltage treatments (p-value > 0.05). The lack of significant variation in capsule diameter suggests that droplet size was predominantly governed by the fixed coaxial nozzle geometry rather than the applied voltage. Accordingly, the optimal operating condition was identified based on capsule morphology, structural integrity of the core–shell system, and overall size uniformity, which are more critical indicators of encapsulation performance.

Table 2 : Capsule characteristics at different voltages (2.0 % w/v alginate).

V (Volt)	Mean size (mm)*	Observation
0	4.3136 ± 0.11[a]	Deformed, no core-shell
500	4.2910 ± 0.07[a]	Partial encapsulation
1,000	4.2774 ± 0.05[a]	Eccentric core
1,500	4.3610 ± 0.22[a]	Optimal: spherical, centered
2,500	4.0364 ± 0.21[a]	Shell rupture, leakage

**Values are presented as the mean ± SD (n = 3). Means sharing the same superscript letters are not significantly different (p-value > 0.05).*

Based on the optimized processing parameters, the resulting capsules exhibited a spherical morphology and good size uniformity, as shown in Figure 5. The average capsule diameter was approximately 4.3 mm, and no visible shell defects were observed. These observations are consistent with the improved core–shell integrity obtained under the selected alginate concentration and applied voltage.

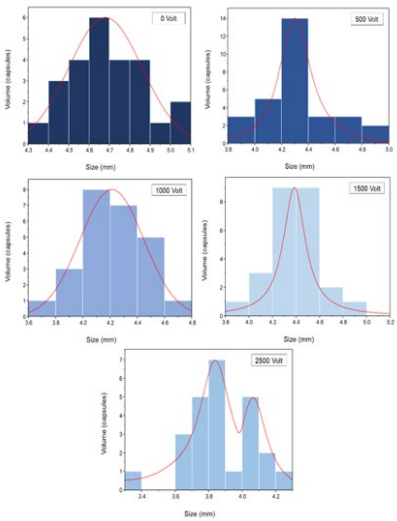

Figure 4 : Size distribution of capsules with 0, 500, 1,000, 1,500, and 2,500 volt.

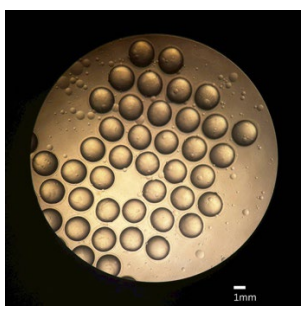

Figure 5: Optical microscopy image of kratom extract-loaded alginate–gelatin core–shell capsules fabricated by coaxial electrospray under the optimized conditions.

3.2 *Structural Characterization*

FT-IR spectra confirmed successful encapsulation via overlapping functional groups of alginate and kratom extract (Figure 6a). The kratom extract displayed characteristic bands at 3,391 cm^{-1} (N–H stretching of amine), 2,926 cm^{-1} (C–H stretching), 1,610 cm^{-1} (C=C aromatic stretching), and 1,029 cm^{-1} (C–O stretching of alcohol/ether). Sodium alginate exhibited a broad O–H stretching at 3,436 cm^{-1}, C=O stretching of carboxylate (COO^-) at 1,615 cm^{-1}, and C–O–C glycosidic bond at 1,070 cm^{-1}. The capsule spectrum displayed superimposed bands from both components: O–H/N–H at 3,425 cm^{-1}, an overlapping C=C/C=O band at 1,637 cm^{-1}, C–O at 1,021 cm^{-1}, and C–O–C at 1,053 cm^{-1} (Table 3).

Table 3 : FT-IR functional group assignments.

Wavenumber (cm^{-1})			Functional Groups
Kratom Leaf Extract	Sodium Alginate	Boba Capsules	
3391.40	-	3425.15	Amine group
2926.06	-	2927.05	C-H (stretching)
-	3435.71	3425.15	Hydroxyl groups
1610.23	-	1637.10	C=C (aromatic stretching)
	1615.07	1637.10	C=O (stretching)
1028.50	-	1021.31	C-O (alcohol and ether stretching)
-	1070.37	1053.23	C-O-C (Stretching)

The concordance of bands confirmed intact encapsulation of the kratom extract within the alginate shell. In addition, UV–Vis analysis showed characteristic absorption at 225 nm corresponding to mitragynine reference standard [19]. Additional peaks at longer wavelengths reflected the complex mixture of alkaloids and secondary metabolites present in the crude extract (Figure 6b).

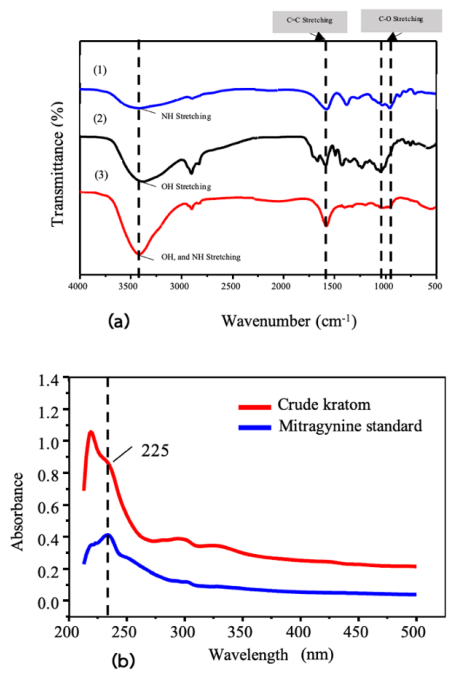

Figure 6: (a) FT-IR spectra of kratom leaf extract (1) and sodium alginate (2) compared with the prepared capsules (3) and (b) UV–Visible spectra of mitragynine extracted from kratom leaves compared with the mitragynine standard.

Applied Science and Engineering Progress, Vol. 20, No. 2, 2027, 8264

3.3 *Stability of boba capsules*

Capsule stability was strongly influenced by environmental pH due to the pH-responsive nature of the calcium–alginate network [10]. As shown in Figure 7, significant differences in capsule size reduction were observed among pH conditions (p-value < 0.05). The percentage size change, used as a quantitative indicator of capsule stability, ranged from 3.94% to 37.77%, demonstrating a strong influence of pH on capsule structural integrity. The greatest shrinkage occurred under strongly acidic conditions, particularly at pH 2 (37.77%), followed by pH 1 (27.29%), where protonation of alginate carboxylate groups and displacement of Ca^{2+} ions weakened the calcium–alginate "egg-box" structure, resulting in network contraction and potential leakage of encapsulated compounds [20]. In contrast, capsules exhibited the highest stability at near-neutral pH, with the smallest size reduction observed at pH 4 (3.94%). The preservation of capsule morphology under pH 4–7 indicates that the calcium–alginate network remained largely intact, supporting potential applications in food, cosmetic, and pharmaceutical systems. Under alkaline conditions (pH 8–10), moderate size reductions were observed, which may be attributed to increased ionization of alginate carboxyl groups, leading to polymer chain relaxation and hydrogel restructuring. Nevertheless, the capsules retained their structural integrity without complete collapse.

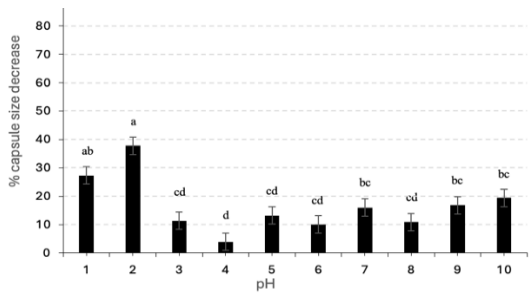

Figure 7: Effect of pH on the percentage size decrease of kratom extract-loaded alginate–gelatin core–shell capsules after 14 days of storage. Data are presented as mean ± standard deviation (SD) from three independent experiments (n = 3). Different lowercase letters above the bars indicate statistically significant differences among pH conditions (p-value < 0.05).

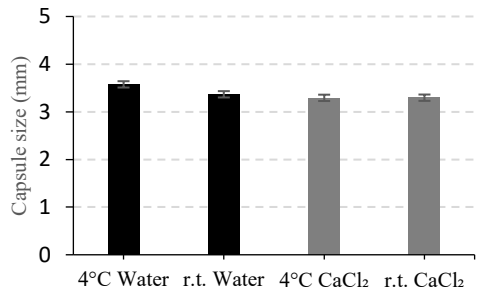

Figure 8 : Size of capsules stored in ultra-pure water and CaCl2 solution at 4 oC and room temperature. Data are presented as mean ± standard deviation (SD) from three independent experiments (n = 3). No statistically significant differences were observed among the storage conditions (p-value > 0.05).

Storage stability studies further demonstrated that the capsules maintained their size and morphology in ultrapure water and calcium chloride solution at both room temperature and 4 °C over 14 days (Figure 8). Statistical analysis revealed no significant differences in capsule size among the storage conditions (p-value > 0.05), indicating good dimensional stability. Although a slight size reduction was observed in calcium chloride solution, likely due to additional ionic crosslinking and network compaction, the overall capsule structure remained intact. The 14-day evaluation was conducted as a preliminary assessment of capsule integrity and environmental resistance, which was sufficient to identify major changes in morphology and stability under the tested conditions. Nevertheless, longer-term studies are required to evaluate shelf-life, active compound retention, and storage performance under practical conditions. These findings demonstrate the robustness of the alginate–gelatin encapsulation system and its suitability as a protective carrier for kratom-derived bioactive compounds.

The developed alginate–gelatin capsules were intended to protect kratom alkaloids, improve storage stability, and facilitate dosage control rather than provide sustained release. The capsule shell is designed to be disrupted during consumption or processing, enabling rapid release of the encapsulated extract. Therefore, controlled-release behavior was not considered a primary performance objective in the present study. Overall, the results demonstrate the robustness of the encapsulation system and its potential as a protective carrier for kratom-derived bioactive compounds.

3.4 *Mitragynine quantification*

GC–MS analysis of the crude kratom extract identified mitragynine at a retention time of 24.365–24.490 min, confirmed by characteristic fragment ions at m/z 397 [M^+], 383 [$M–CH_3]^+$, and 214 [M–loss of ester group]$^+$ [12], [21]. Peak area integration indicated that mitragynine constituted approximately 9% of the total extract. A UV–Vis calibration curve at 225 nm showed excellent linearity over 5–25 ppm ($y = 0.0225x − 0.0616$, $R^2 = 0.9993$). Analysis of an ethanol solution prepared from 10 capsules yielded an absorbance of 0.0916, corresponding to a total extract concentration of 6.8089 ppm (0.0068 mg/mL). Based on the GC–MS-derived mitragynine fraction, the mitragynine content was calculated to be 0.000612 mg per 10 capsules, or 0.0000612 mg per capsule. Although the mitragynine loading was relatively low, the primary objective of this study was to establish the feasibility of kratom extract encapsulation using an alginate–gelatin coaxial electrospray system rather than to develop a therapeutically optimized dosage form. The low loading level likely resulted from the conservative extract concentration and processing conditions employed to maintain stable capsule formation and preserve capsule integrity during electrospray processing. While the developed system successfully demonstrated incorporation of kratom extract while maintaining favorable morphology, stability, and cytocompatibility, the measured mitragynine content indicates that many capsules would be required to achieve therapeutically relevant intake levels. Therefore, substantial improvement in loading capacity and encapsulation efficiency will be necessary before practical pharmaceutical application can be considered. Future studies should focus on increasing extract concentration, optimizing the core-to-shell ratio and electrospray parameters, and utilizing more concentrated kratom fractions or purified mitragynine to enhance loading efficiency while maintaining capsule quality.

3.5 *Cytotoxicity*

The MTT assay demonstrated that crude kratom extract concentrations of 0–10 µg/mL maintained Vero cell viability above 85% and consistently above the 80% cytocompatibility threshold, indicating no significant cytotoxic effects (Figure 9a). Cell viability remained close to 95–100% at lower concentrations (0.3125–2.5 µg/mL), with only a slight decrease observed at higher concentrations (5–10 µg/mL). The dose–response profile showed a concentration-dependent reduction in viability, with an IC_{50} value of 32.47 µg/mL (Figure 9b), which is substantially higher than the tested concentration range and suggests a wide safety margin under the experimental conditions. These findings indicate low toxicity of the kratom extract toward normal epithelial cells. Although previous studies have reported IC_{50} values of mitragynine in neuronal cell lines in the range of 75–80 µM [22], direct comparison should be interpreted with caution because cytotoxic responses are highly dependent on cell type, experimental conditions, and the tested material (pure mitragynine versus crude extract). Therefore, the present results primarily demonstrate the cytocompatibility of the developed formulation in Vero cells rather than providing a direct assessment of neuronal safety. Overall, the absence of significant cytotoxicity under the tested conditions supports the potential application of this encapsulation system in food and pharmaceutical delivery systems.

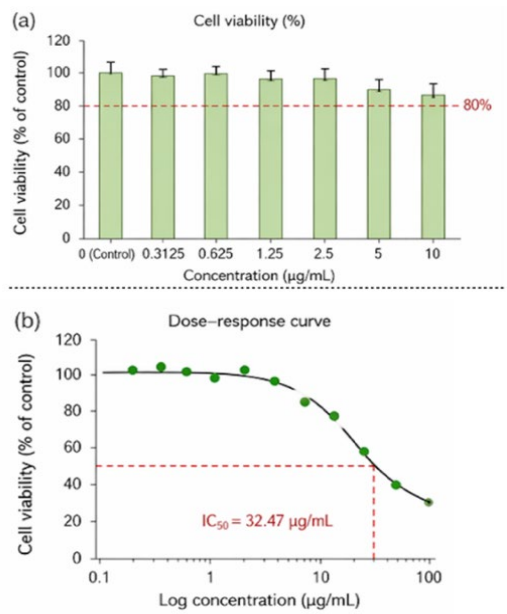

Figure 9: (a) Cytotoxicity of Kratom extract on Vero cell and (b) Dose-response curve.

4 Conclusion

This study successfully developed kratom extract–loaded alginate–gelatin boba capsules using a coaxial electrospray technique under optimized conditions of 2.0 % (w/v) sodium alginate and an applied voltage of 1,500 V. The optimized process produced spherical capsules with uniform size distribution (4.29 mm) and a well-defined core–shell structure. FT-IR analysis confirmed successful encapsulation of the kratom extract, while the developed capsules exhibited good structural stability under neutral pH and varying storage temperature conditions. Cytotoxicity evaluation using Vero cells demonstrated no significant toxicity within the tested concentration range, indicating acceptable preliminary biocompatibility of the developed system. Although the mitragynine loading capacity obtained in the present study was relatively low for practical therapeutic applications, the results demonstrate the feasibility of using coaxial electrospray as a mild and controllable encapsulation platform for kratom-derived bioactive compounds. Future studies should focus on improving loading efficiency through optimization of extract concentration, core-to-shell ratio, capsule size, and electrospray processing parameters, as well as the use of more concentrated kratom fractions or purified mitragynine. Overall, the findings highlight the potential of this scalable, single-step encapsulation approach for future applications in functional foods, nutraceuticals, and pharmaceutical delivery systems.

Acknowledgement

The authors would like to thank the Department of Industrial Chemistry, Faculty of Applied Science, KMUTNB, for providing the laboratory facility. We also appreciate the assistance of Dr. Chanikan Sonklin for the cytotoxicity test.

Author Contributions

C.T.: investigation, research design, data analysis and writing an original draft; A.S.: investigation, research design; L.S.: research design, data analysis; S.S.: research design, data analysis; I.S.: writing—reviewing and editing N.T.: conceptualization, methodology, data curation, writing—reviewing and editing, funding acquisition, project administration. All authors have read and agreed to the published version of the manuscript.

Conflicts of Interest

The authors declare no conflict of interest.

Declaration of generative AI and AI-assisted technologies in the writing process

The authors utilized the ChatGPT tool to enhance the language and readability of the manuscript.

References

[1] A. H. Beckett, E. J. Shellard, J. D. Phillipson, and C. M. Lee, "The *Mitragyna* species of Asia—Part. VII: Indole alkaloids from the leaves of *Mitragyna speciosa* Korth.," *Planta Medica*, vol. 14, no. 3, pp. 277–288, Aug. 1966, doi: 10.1055/s-0028-1100055.

[2] T. Karunakaran, K. Z. Ngew, A. A. D. Zailan, V. Y. Mian Jong, and M. H. Abu Bakar, "The chemical and pharmacological properties of mitragynine and its diastereomers: An insight review," *Frontiers in Pharmacology*, vol. 13, Art. no. 805986, Feb. 2022, doi: 10.3389/fphar.2022.805986.

[3] H. Takayama, "Chemistry and pharmacology of analgesic indole alkaloids from the rubiaceous plant, *Mitragyna speciosa*," *Chemical and Pharmaceutical Bulletin*, vol. 52, no. 8, pp. 916–928, Aug. 2004, doi: 10.1248/cpb.52.916.

[4] K. Matsumoto et al., "Inhibitory effect of mitragynine, an analgesic alkaloid from Thai herbal medicine, on neurogenic contraction of the vas deferens," *Life Sciences*, vol. 78, no. 2, pp. 187–194, Nov. 2005, doi: 10.1016/j.lfs.2005.04.042.

[5] L. Zhang, J. Huang, T. Si, and R. X. Xu, "Coaxial electrospray of microparticles and nanoparticles for biomedical applications," *Expert Review of Medical Devices*, vol. 9, no. 6, pp. 595–612, Nov. 2012, doi: 10.1586/erd.12.58.

[6] G. I. Taylor, "Disintegration of water drops in an electric field," *Proceedings of the Royal Society of London A: Mathematical, Physical and Engineering Sciences*, vol. 280, no. 1382, pp.383–397, Jul. 1964, doi: 10.1098/rspa.1964.0151.

[7] A. Shalapy et al., "Adsorption of deoxynivalenol (DON) from corn steep liquor (CSL) by the microsphere adsorbent SA/CMC loaded with

calcium," *Toxins*, vol. 12, no. 4, Art. no. 208, Mar. 2020, doi: 10.3390/toxins12040208.

[8] P. R. Patel and D. Haemmerich, "Review on electrospray nanoparticles for drug delivery: Exploring applications," *Polymers for Advanced Technologies*, vol. 35, no. 7, Art. no. e6507, Jul. 2024, doi: 10.1002/pat.6507.

[9] N. Hani, M. H. Azarian, A. E. Torkamani, and W. A. K. Mahmood, "Characterisation of gelatin nanoparticles encapsulated with *Moringa oleifera* bioactive extract," *International Journal of Food Science & Technology*, vol. 51, no. 11, pp. 2327–2337, Nov. 2016, doi: 10.1111/ijfs.13211.

[10] K. Y. Lee and D. J. Mooney, "Alginate: Properties and biomedical applications," *Progress in Polymer Science*, vol. 37, no. 1, pp. 106–126, Jan. 2012, doi: 10.1016/j.progpolymsci.2011.06.003.

[11] S. Zhao et al., "Coaxial electrospray of liquid core-hydrogel shell microcapsules for encapsulation and miniaturized 3D culture of pluripotent stem cells," *Integrative Biology*, vol. 6, no. 9, pp. 874–884, Sep. 2014, doi: 10.1039/C4IB00100A.

[12] M. C. Gómez-Guillén, B. Giménez, M. E. López-Caballero, and M. P. Montero, "Functional and bioactive properties of collagen and gelatin from alternative sources: A review," *Food Hydrocolloids*, vol. 25, no. 8, pp. 1813–1827, Dec. 2011, doi: 10.1016/j.foodhyd.2011.02.007.

[13] B. Sarker et al., "Fabrication of alginate–gelatin crosslinked hydrogel microcapsules and evaluation of the microstructure and physico-chemical properties," *Journal of Materials Chemistry B*, vol. 2, no. 11, pp. 1470–1482, Mar. 2014, doi: 10.1039/C3TB21509A.

[14] C. Citti, A. Laganà, A. L. Capriotti, C. M. Montone, and G. Cannazza, "Kratom: The analytical challenge of an emerging herbal drug," *Journal of Chromatography A*, vol. 1703, Art. no. 464094, Aug. 2023, doi: 10.1016/j.chroma.2023.464094.

[15] A. C. Kruegel and O. Grundmann, "The medicinal chemistry and neuropharmacology of kratom: A preliminary discussion of a promising medicinal plant and analysis of its potential for abuse," *Neuropharmacology*, vol. 134, Pt. A, pp. 108–120, May 2018, doi: 10.1016/j.neuropharm.2017.08.026.

[16] S. N. A. Syed Azhar et al., "Screening and selection of formulation components of nanostructured lipid carriers system for *Mitragyna speciosa* (Korth). Havil. drug delivery," *Industrial Crops and Products*, vol. 198, Art. no. 116668, Aug. 2023, doi: 10.1016/j.indcrop.2023.116668.

[17] S. D. Sarker and L. Nahar, "Formulation and Delivery of Mitragynine: A Mini Review," *Journal of Medicinal Natural Products*, vol. 2, no. 3, Art. no. 100020, Sep. 2025, doi: 10.53941/jmnp.2025.100020.

[18] A. Jaworek, A. T. Sobczyk, "Electrospraying route to nanotechnology : an overview", *Journal of Electrostatics*, vol. 66, no. 3–4, pp. 197–219, Mar. 2008, doi: 10.1016/j.elstat.2007.10.001.

[19] A. C. Kruegel et al., "Synthetic and receptor signaling explorations of the *Mitragyna* alkaloids: Mitragynine as an atypical molecular framework for opioid receptor modulators," *Journal of the American Chemical Society*, vol. 138, no. 21, pp. 6754–6764, May 2016, doi: 10.1021/jacs.6b00360.

[20] H. Malektaj, A. D. Drozdov J. deClaville Christiansen, "Swelling of Homogeneous Alginate Gels with Multi-Stimuli Sensitivity", *International Journal of Molecular Sciences*, vol. 24, no. 6, Art. no. 5064, Mar. 2023, doi: 10.3390/ijms24065064.

[21] D. Ponglux et al., "A new indole alkaloid, 7α-hydroxy-7H-mitragynine, from *Mitragyna speciosa* in Thailand," *Planta Medica*, vol. 60, no. 6, pp. 580–581, Dec. 1994, doi: 10.1055/s-2006-959578.

[22] N. A. Saidin, E. Holmes, H. Takayama, and N. J. Gooderham, "The cellular toxicology of mitragynine, the dominant alkaloid of the narcotic-like herb, *Mitragyna speciosa* Korth," *Toxicology Research*, vol. 4, no. 5, pp. 1173–1183, Jun. 2015, doi: 10.1039/C5TX00113G